Nano Research 2016, 9(10): 3084–3092
DOI 10.1007/s12274-016-1191-x
Research Article
ISSN 1998-0124
CN 11-5974/O4

pH-controlled DNAzymes: Rational design and their applications in DNA-machinery devices

Yuqi Chen[1], Yanyan Song[1], Zhiyong He[1], Zijing Wang[1], Wenting Liu[1], Fuan Wang[1], Xiaolian Zhang[2], and Xiang Zhou[1] (✉)

[1] *College of Chemistry and Molecular Sciences, The Institute for Advanced Studies, Wuhan University, Wuhan 430072, China*
[2] *School of Medicine, Wuhan University, Wuhan 430071, China*

Received: 1 April 2016
Revised: 17 June 2016
Accepted: 21 June 2016

KEYWORDS
pH,
iMNAzyme,
TNAzyme,
DNA walker,
DNA tetrahedron

ABSTRACT

The availability and reliability of strategies for molecular biosensing over a finely adjustable dynamic range is essential to enhance the understanding and control of vital biological process. To expand the versatility and utility of nucleic acid-related enzymes, we demonstrated a rational approach to acquiring tunable, pH-dependent deoxyribozymes (DNAzymes) with catalytic activities and response sensitivities that can be tuned through a simple change in solution pH. To do this, we capitalized upon the pH dependence of Hoogsteen interactions and designed i-motif- and triplex-based DNAzymes that can be finely regulated with high precision over a physiologically relevant pH interval. The modified DNAzymes are dependent upon pH for efficient cleavage of substrates, and their catalytic performance can be tuned by regulating the sequence of inserted i-motif/triplex structures. The principle of tunable, pH-dependent DNAzymes provides the opportunity to engineer pH-controlled DNA-machinery devices with unprecedented sensitivity to pH changes. For example, we constructed a DNA-walker device, the stepping rate of which could be adjusted by simply modulating solution pH within an interval of 5.6 to 7.4, as well as a DNA tetrahedron that can be opened at pH 6.4 and kept closed at pH 7.4. The potential of this approach is not limited to serve as pH-dependent devices, but rather may be combined with other elements to expand their practical usefulness.

1 Introduction

Deoxyribozymes (DNAzymes) are DNA molecules capable of catalyzing a wide range of chemical reactions, such as RNA cleavage, DNA cleavage, DNA ligation, RNA ligation, DNA phosphorylation, thymine dimer repair, porphyrin metalation, and DNA deglycosylation [1–9]. Due to their easy construction, high efficiency, and good maneuverability, DNAzymes are of growing interest in the field of DNA nanotechnology, bio-analysis, and targeted therapy [10–12]. To extrapolate the versatility of DNAzymes, many studies were

Address correspondence to xzhou@whu.edu.cn

devoted to modifying their structure and function [13–15]. Because pH changes represent important signals in biological pathways that affect physical health [16], we concentrated on the development of novel DNAzymes with catalytic performance capable of being modulated by pH.

Inspired by a multicomponent nucleic acid enzyme (MNAzyme)-design strategy [17], here, we designed two tunable, pH-dependent DNAzyme strategies: the i-motif structure-based nucleic acid enzyme (iMNAzyme) strategy and the triplex structure-based nucleic acid enzyme (TNAzyme) strategy (Fig. 1), both exhibiting catalytic performance that can be tuned by simply regulating the pH of the reaction conditions. The basic design method was to split the catalytic core of a DNAzyme and then link the partzymes by an i-motif or DNA triplex-structure sequence. We envisioned that the catalytic activities and response sensitivities of the iMNAzyme/TNAzyme could be tunable by virtue of PH-dependent transformations of the i-motif and triplex.

An i-motif is a four-stranded DNA secondary structure that can be formed from cytosine sequences and stabilized by acidic conditions through intercalated cytosine-cytosine (+) base pairs and will transform into random coil conformations due to the deprotonation of cytosines at higher pH [18]. A DNA triplex is formed when pyrimidine or purine bases occupy the major groove of a B-form DNA double helix forming Hoogsteen or reversed-Hoogsteen hydrogen bonds with purines of the Watson–Crick base pairs. The recognition of guanidine requires the cytosine in the third strand to be pronated; therefore, triplex formation will only work under certain low-pH conditions [19]. We hypothesized that both of these structures would be suitable scaffolds for ultra-sensitive,

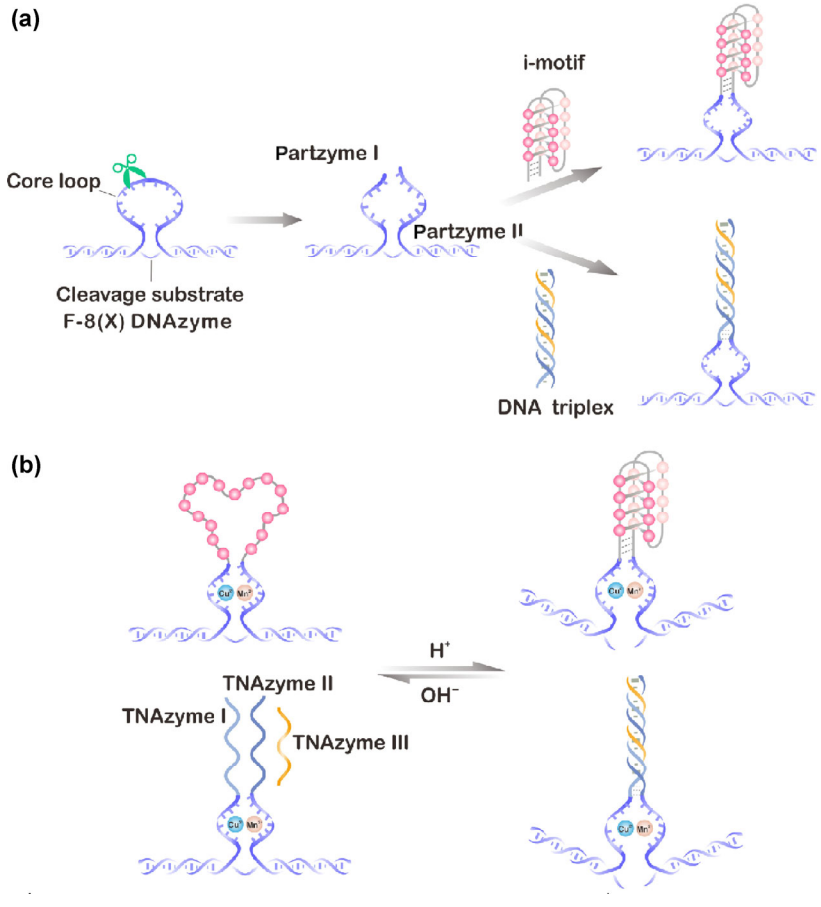

Figure 1 Design principle of the (a) iMNAzyme and (b) TNAzyme. A schematic shows their construction and pH-guided assembly/disassembly. Substrates cleaved by an assembled iMNAzyme/TNAzyme in the presence of cofactors (Mn^{2+} and Cu^{2+}) under appropriate pH conditions.

pH-controlled DNAzyme design, because they possess two essential characteristics: (1) structure transformation with high pH-response sensitivity, and (2) the capacity to undergo a transition over the physiological pH interval. Therefore, the introduction of an i-motif/triplex structure might allow for better control and a tunable, pH-triggered DNAzyme over a physiological pH range. Since pH change is capable of being manipulated and often associated with different diseases (e.g., pH deregulation is emerging as an important hallmark of cancer) [16], i-motif/triplex structures could be accessible for developing pH-response DNA machinery and drug-releasing DNA nanostructures at specific pathology associated pH values.

The design principle for the iMNAzyme/TNAzyme is illustrated in Fig. 1, with both constructed on the split DNAzyme F-8(X), which is a Mn^{2+}- and Cu^{2+}-dependent DNAzyme reported by Tang [20] that can efficiently catalyze nucleotide excision at a thymine (T)-containing DNA substrate with a catalytic rate of 0.0487 h^{-1}. The iMNAzyme is composed of two partial enzymes (partzymes I and II) split from F-8(X) that are directly linked by an i-motif sequence to form the integral iMNAzyme (Fig. 1(a)), while the TNAzyme is composed of three partzymes: TNAzyme I, II, and III. The inserted DNA triplex structure can be assembled to form a complete TNAzyme in the presence of an additional single-stranded TNAzyme III with TNAzyme I and II (Fig. 1(b)). Partzymes I and II of iMNAzyme/TNAzyme contain two domains, including substrate-recognition arms that bind substrate and partial catalytic core sequences engineered by splitting the catalytic core of F-8(X) into two parts. Upon i-motif-/triplex-structure assembly and stability under lower pH conditions, partzymes I and II are pulled closer and then combined to create a complete catalytic core. In contrast, i-motif/triplex structures are disassembled under higher pH conditions, resulting in partzyme separation and destruction of the catalytic core. We hypothesized that the iMNAzyme/TNAzyme could catalyze substrate cleavage under lower pH conditions based on the assembly of the catalytic core, whereas its catalytic activity would be rapidly weakened at higher pH conditions.

2 Results and discussion

First, we tested the iMNAzyme to verify the feasibility of our approach. Based on our strategy, we designed one iMNAzyme (iMNAzyme-3), with partzymes split from G_7 and C_8 sites of F-8(X). The sequences are shown in Table S1 in the Electronic Supplementary Material (ESM). The polyacrylamide gel results (Fig. S2 in the ESM) demonstrated that the iMNAzyme cleaved the fluorophore (FAM)-labelled DNA substrate LS-1 in a similar fashion to the original DNAzyme, indicating that the reconstructed iMNAzyme retained adequate catalytic activity. iMNAzymes with partzymes split at three other possible positions (iMNAzyme-3-2 ($C_9{}^{\downarrow}G_{10}$), iMNAzyme-3-3 ($A_5{}^{\downarrow}T_6$), and iMNAzyme-3-4 ($C_{15}{}^{\downarrow}G_{16}$)) were also tested (Fig. S3 in the ESM), but all displayed negligible catalytic activities. This was likely due to the catalytic core structure being destroyed by the inserted i-motif or interfered due to increased steric hindrance.

Next, we optimized the Mn^{2+} and Cu^{2+} requirements for optimal catalytic activity, with Mn^{2+} and Cu^{2+} concentrations necessary for optimal cleavage measured at 20 mM and 12.5 μM, respectively (Fig. S4 in the ESM). These optimization conditions were used for all further experiments.

We then investigated the reaction kinetics, obtaining cleavage rates (k_{obs}) of ~0.0533 h^{-1}, with the catalytic efficiency of iMNAzyme-3 only slightly decreased as compared to that of the DNAzyme on which it was based (Fig. S5(a) in the ESM). To accelerate the reaction rate, 100 μM H_2O_2 was added to the reaction system [9], with the observed k_{obs} increasing to 0.0489 min^{-1} (65-fold increase), indicating that the reaction can be almost completed in just 40 min (Fig. S5(b) in the ESM). These data demonstrated that iMNAzyme-3 could function as a feasible DNAzyme capable of cleaving DNA substrates with high efficiency.

To estimate the effective catalytic pH range and the potential to tune response sensitivity, we evaluated the catalytic activity of iMNAzyme-3 over the physiological pH range within an interval from 5.6 to 7.8. As expected, this construction rendered iMNAzyme-3 dependent upon pH for efficient cleavage (Fig. S6 in the ESM). iMNAzyme-3 was inactive at pH 5.6, but exhibited the highest activity at pH 6.4. Above this

pH, catalytic activity rapidly deceased, from pH 6.4 to pH 7.8. This strategy delivered a DNAzyme with a cleavage transition at pH 6.4 (0.2-unit precision) and with a total of 2.0 pH-unit response range. Both the i-motif insertion and the DNAzyme itself influenced this cleavage behavior. Higher pH levels resulted in dissembled i-motif structure, resulting in destruction of the catalytic core, whereas lower pH levels reduced the catalytic activity of the DNAzyme (Fig. S7(a) in the ESM). Because the catalytic activity of F-8(X) was also decreased by lower pH, we estimated the influence of the inserted i-motif in part by comparing the catalytic activity of iMNAzyme-3 with the original F-8(X) (Fig. S7(a) in the ESM). A subtraction method was used to obtain a result (Fig. S7(b) in the ESM) that showed increased interference of the inserted i-motif sequence upon increases in pH. Furthermore, the catalytic activity of iMNAzyme-3 could be altered repeatedly by converting solution pH (Fig. S8 in the ESM). Similarly, one TNAzyme was constructed (TNAzyme-2) and verified as a tunable, pH-dependent DNAzyme in addition to iMNAzyme-3. When three partzymes were present simultaneously, no catalytic activity was observed when TNAzyme-3 was removed from the reaction solution. TNAzyme-2 exhibited a cleavage transition at pH 7.0, and nearly ceased to be effective at pH 5.6 and 7.6 (Fig. S9 in the ESM). These results suggested the possibility of "fine-tuning" the catalytic performance of DNAzymes over a physiological pH interval by the insertion of an i-motif/triplex sequence into the catalytic core of an original DNAzyme.

To estimate the potential to tune iMNAzyme catalytic performance, we investigated the effects of the following characteristics: (1) base pairs connecting the i-motif structure and the catalytic core (Fig. 2(a)), (2) the number of cytosine layers (Fig. 2(d)), and (3) the sequence of the i-loop (Fig. 2(g)) on catalytic activity and the cleavage-transition pH point. The results highlighted qualitative trends, including that iMNAzyme cleavage activities can be significantly promoted by longer connections between base pairs (iMNAzyme-4 > iMNAzyme-3 > iMNAzyme-2 > iMNAzyme-0), more cytosine layers (iMNAzyme-2-6C > iMNAzyme-2-5C > iMNAzyme-2-4C > iMNAzyme-2-3C), and i-loops containing more thymines (iMNAzyme-2-4C-TTT > iMNAzyme-2-4C-ATT > iMNAzyme-2-4C-AAT > iMNAzyme-2-4C-AAA) (Figs. 2(b), 2(e), and 2(h)). Additionally, iMNAzymes with longer connections between base pairs have a lower cleavage-transition pH (Fig. 2(c), Fig. S10(a) in the ESM, iMNAzyme-0 ≈ iMNAzyme-2 > iMNAzyme-3 ≈ iMNAzyme-4, translated from pH 6.6 to 6.4); however, the cleavage-transition pH decreased for iMNAzymes containing more cytosine layers (Fig.2(f), Fig. S10(b) in the ESM, iMNAzyme-2-3C ≈ iMNAzyme-2-4C < iMNAzyme-2-5C ≈ iMNAzyme-2-6C, translated from pH 6.4 to 6.6), and i-loops containing more Ts (Fig. 2(i), Fig. S10(c) in the ESM, iMNAzyme-2-4C-AAA < iMNAzyme-2-4C-AAT < iMNAzyme-2-4C-ATT < iMNAzyme-2-4C-TTT, translated from pH 5.6 to 6.4). The most remarkable influencing factor was the sequence of the i-loop. We predicted that the probable reason for the shift in transition pH point was due to the different stabilities associated with the i-motif structures, i.e., the more stable the i-motif structure, the easier its formation; therefore, it maintained a higher transition point, because it was able to be stabilized under higher pH conditions.

We then estimated the potential tunability of TNAzyme catalytic performance. We investigated the effects of the following characteristics: (1) base pairs connecting the DNA triplex structure and catalytic core (Figs. 3(a)–3(c)) and (2) relative content of CGC/TAT triplets in the triplex structure (Figs. 3(d)–3(f)). The results highlighted qualitative trends, including promotion of TNAzyme-related cleavage activities by longer connections between base pairs (TNAzyme-3 > TNAzyme-2 > TNAzyme-1 > TNAzyme-0) and lower relative content of CGC/TAT triplets (TNAzyme-2-0.5 > TNAzyme-2-0.6 > TNAzyme-2-0.7 > TNAzyme-2-0.8) (Figs. 3(b) and 3(e)). Additionally, the cleavage-transition pH increased for TNAzymes with longer connections between base pairs (Fig. 3(c), Fig. S11(a) in the ESM, TNAzyme-3 ≈ TNAzyme-2 > TNAzyme-1 > TNAzyme-0, translated from pH 7.0 to 6.4) and a higher relative content of CGC/TAT triplets (Fig. 3(f), Fig. S11(b) in the ESM, TNAzyme-2-0.5 > TNAzyme-2-0.6 > TNAzyme-2-0.7 > TNAzyme-2-0.8, translated from pH 6.6 to 7.2).

A series of efficient iMNAzymes/TNAzymes exhibiting different catalytic transition pH points

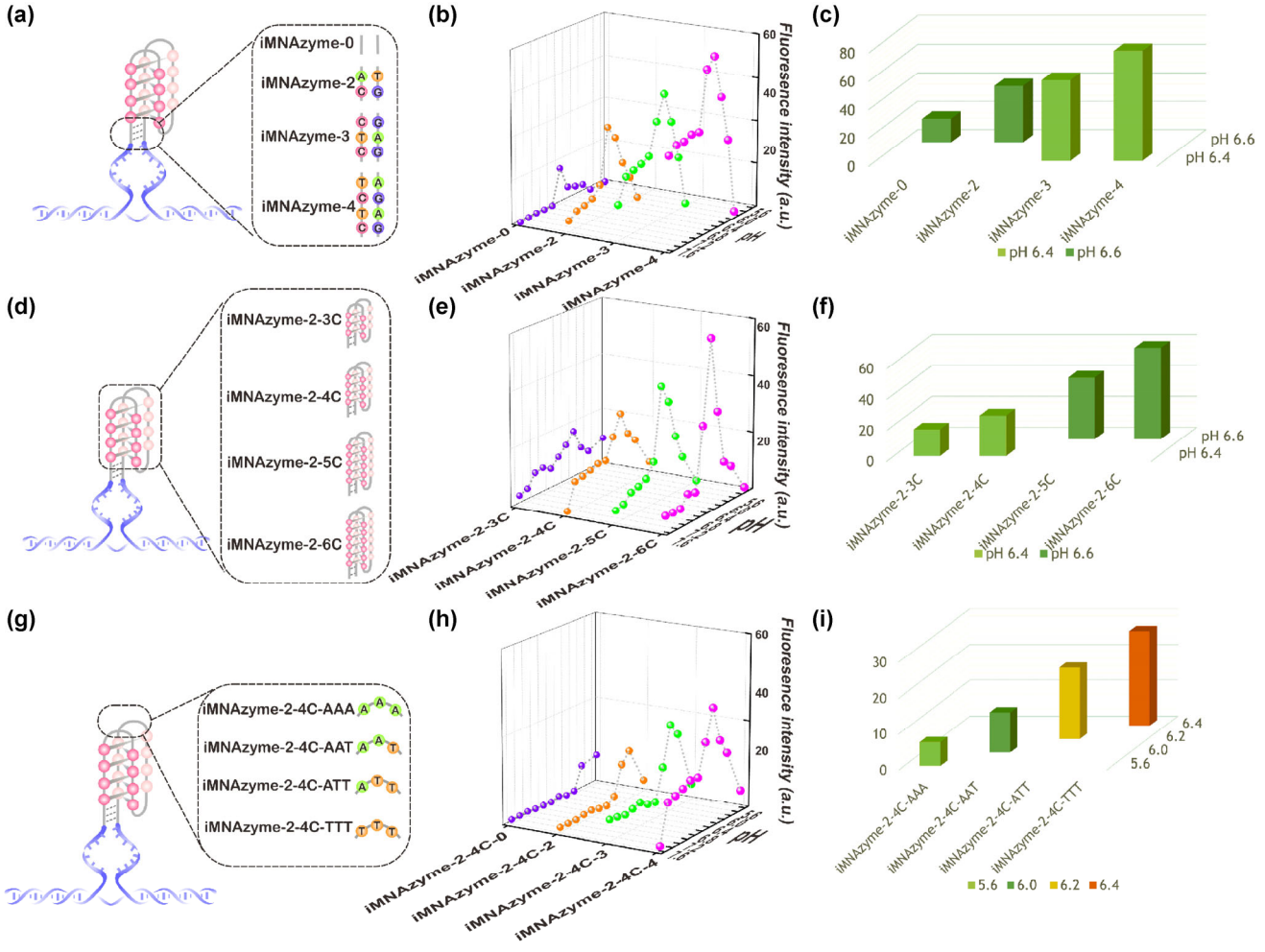

Figure 2 Catalytic activities and cleavage-transition pH points of iMNAzymes can be tuned via manipulation of (a)–(c) base pairs connecting the i-motif structure and the catalytic core, (d)–(f) the number of cytosine layers, and (g)–(i) the loop sequence of the i-motif structure. (a), (d), and (g) Schematic describing the sequence tuning of the iMNAzyme. (b), (e), and (h) Catalytic activities of the iMNAzyme at different pH points over the physiological pH interval ranging from pH 5.6 to 7.8. Experiments were performed at pH 5.6, 6.0, 6.2, 6.4, 6.6, 6.8, 7.0, 7.2, 7.4, 7.6, and 7.8. (c), (f), and (i) Histogram represents the maximum catalytic yield and cleavage-transition pH points for the iMNAzyme.

ranging from pH 5.6 to 7.2 were constructed (Fig. S12(a) in the ESM). To estimate the response sensitivities, we compared the ratio of their best cleavage yield to that observed under pH 7.4. Our results revealed that it was unequal, ranging from to 1.7 to 84.6 (Fig. S12(b) in the ESM). Among all constructed iMNAzymes/TNAzymes, TNAzyme-3 showed significant catalytic behavior, because it exhibited both good catalytic efficiency (catalytic yield at ~60% over 10 h without the addition of H_2O_2) and response sensitivity (cleavage yield at pH 6.6 nearly 50-fold larger than that observed at pH 7.4).

Here, for the first time, we demonstrated how the incorporation of an i-motif/triplex structure along with sequence manipulation could tune DNAzyme catalytic performance. The unique advantage of the i-motif-/triplex-based systems reported here is their capability to simultaneously tune catalytic transition, activity, and response sensitivity with high precision. According to the existing qualitative results, it was possible to construct DNAzymes owning specific catalytic behaviors for different uses.

To expand the functionality of the tunable, pH-dependent DNAzyme, we used the iMNAzyme to construct a DNA-walker device with a stepping rate adjustable by simply modulating solution pH

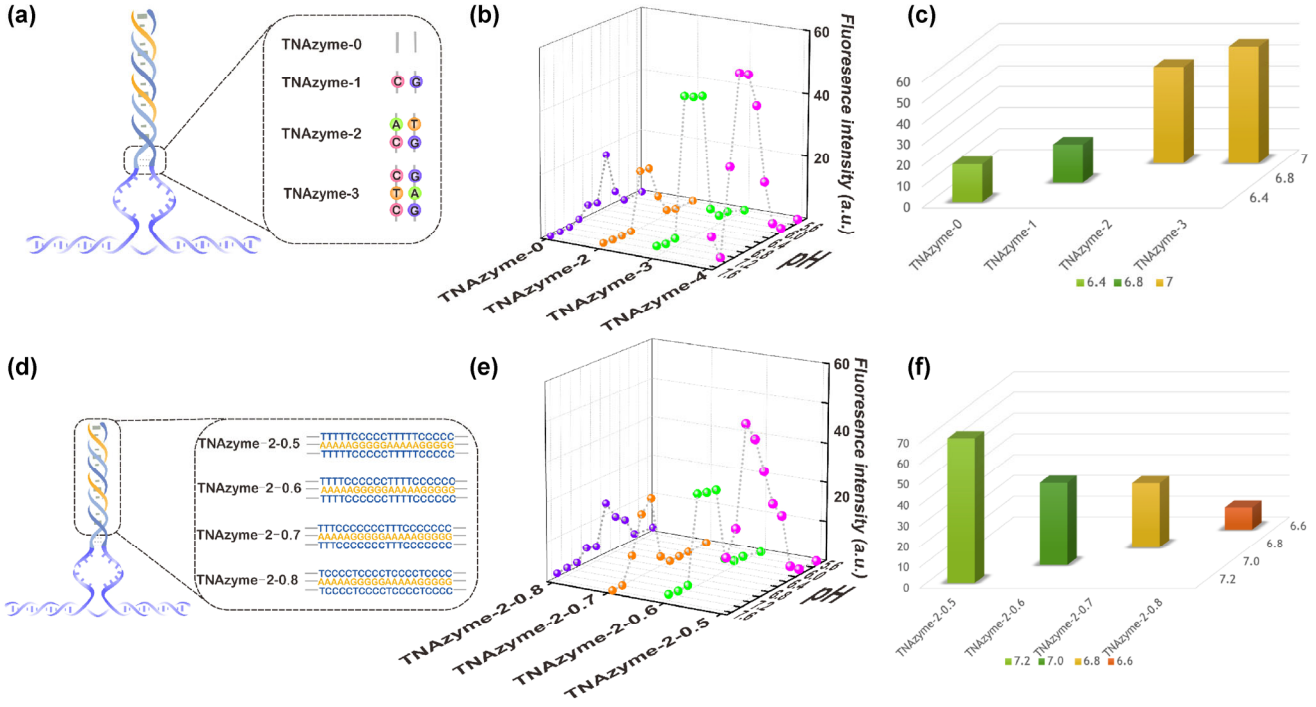

Figure 3 Catalytic activities and cleavage-transition pHs of TNAzymes can be tuned via manipulation of (a)–(c) base pairs connecting the triplex structure and the catalytic core and (d)–(f) the relative content of CGC/TAT triplets in the triplex structure. (a) and (d) Schematic describing the sequence tuning of the TNAzyme. (b) and (e) Catalytic activities of the TNAzyme at different pH points over the physiological pH interval ranging from pH 5.6 to 7.6. Experiments were performed at pH 5.6, 6.0, 6.2, 6.4, 6.6, 6.8, 7.0, 7.2, 7.4, and 7.6. (c) and (f) The histogram of maximum catalytic yield and catalytic transition pH point for the TNAzyme.

within an interval of pH 5.6 to 7.4, as well as a DNA tetrahedron that could be opened at pH 6.4 and closed at pH 7.4.

2.1 Novel pH-driven DNA walker

A DNA-walker device is a DNA-mechanical device that uses a DNA fragment to serve as a walker to translocate directionally along a one-dimensional DNA track from station to station [21, 22]. Here, we constructed one of the first DNA walkers with a stepping speed capable of regulation through a simple change in solution pH by introducing our tunable, pH-dependent DNAzyme to perform the walk. Considering maneuverability, the iMNAzyme was chosen to act as i-MNAzyme based walker (iE) rather than the TNAzyme, because the TNAzyme needs three partzymes, which increased the complexity of the walking system. Figure 4 depicts the iMNAzyme-based DNA-walker system. The sequences, construction, and mechanism of the iMNAzyme-based DNA walker are illustrated in the ESM. Once Cu^{2+} and Mn^{2+} are added to the walking buffer at the appropriate pH, the catalytic activity was restored and the movement initiated. We hypothesized that weak acidic conditions would induce the formation of a complete iMNAzyme walker that allowed procession in the appropriate direction (green traffic light); otherwise, the walker would be retarded (red traffic light) at a higher or lower pH due to the disassembly of the i-motif or loss of iMNAzyme catalytic activity. An optical iMNAzyme that functions as a walker should consist of both good response sensitivity and high catalytic efficiency. Considering this, we used iMNAzyme-2-6C as the walker iE, because it was able to reach ~60% cleavage yield at pH 6.6 and show appropriate response sensitivity (the cleavage yield at pH 6.6 was ~12-fold larger than that observed at pH 7.4).

The DNA walker was purified and verified by native polyacrylamide gel electrophoresis (Fig. S13 in the ESM). We observed that the constructed iE performed similar cleavage behavior as that of iMNAzyme-2-6C (Fig. S14 in the ESM). Based on

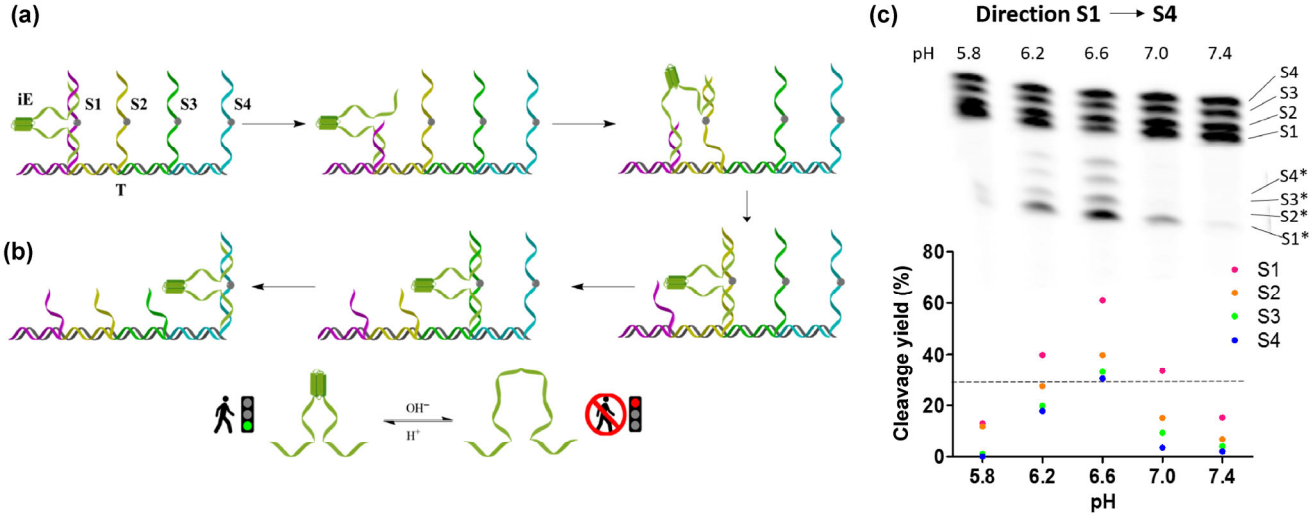

Figure 4 (a) and (b) Overview of the iMNAzyme-based pH-responsive DNA-walker system. (c) Denatured polyacrylamide gel electrophoresis analysis and cleavage-fraction quantification of walker movement.

these results, five pH values (5.8, 6.2, 6.6, 7.0, and 7.4) were chosen to verify the feasibility of the constructed pH-responsive DNA walker. The movement of the iE walker was demonstrated by monitoring the differential cleavage behaviors of the DNA substrate. As seen in Fig. 4(c), sequential cleavage was observed according to the appearance of short, cleaved substrate-fragment bands (S1*, S2*, S3*, and S4*). The overall cleavage yields were S1 > S2 > S3 > S4, indicating that iE moved from S1 to S2 to S3 and, finally, to S4. Additionally, the cleavage yields at pH 6.6 were higher than those observed at pH 6.2 and pH 7.0, while no obvious cleaved-substrate fragments were observed at pH 5.8 or pH 7.4. This indicated that iE could pass unobstructed through the stations at pH 6.6, slow down at pH 6.2 and pH 7.0, and be nearly blocked at pH 5.8 and pH 7.4. We determined that the walker successfully stepped over one station if it cleaved the substrate with >30% cleavage yield (dashed line in Fig. 4(c)). Therefore, at pH 6.6, the iE walker could step from S1 to S4. However, it walks over S1 at pH 6.2 and pH 7.0, and nearly remains *in situ* at pH 5.8 and 7.4. These results illustrated that iE migrated fastest at pH 6.6, and its walking process was seriously obstructed by adjustment of only 0.4 pH units. By choosing the proper iE sequence, we believe that the walking behavior could be extrapolated to cover different pH ranges and stepping rates.

2.2 iMNAzyme-based DNA tetrahedron

A DNA tetrahedron is a DNA nanocage that possesses remarkable nuclease resistance and is capable of entering live mammalian cells [23]. It has been successfully employed for efficient delivery and release of encapsulated drugs by cage disassembly or changing conformations with certain environmental cues [24]. Our strategy was to replace one side of a dsDNA chain with an iMNAzyme and its substrate in order to allow the catalytic reaction to cleave one side, resulting in opening of the DNA tetrahedron (Fig. 5(a)). Native polyacrylamide gel electrophoresis indicated that our DNA tetrahedron was 40% dissembled at pH 6.4, while remaining intact at pH 7.4 (Fig. 5(b)). Compared with many other nanosturctural switching methods [25, 26], our method cannot be reversed; however, it remains sensitive, easy to operate, and does not require additional reagents. Because pH changes are often associated with different diseases, this method could be useful to activate the functionality of drug-releasing DNA nanomachines at specific pH values.

3 Conclusions

Here, we described a strategy to modulate the cleavage performance of DNAzymes by regulating the solution pH. This tuning is accomplished by incorporating one

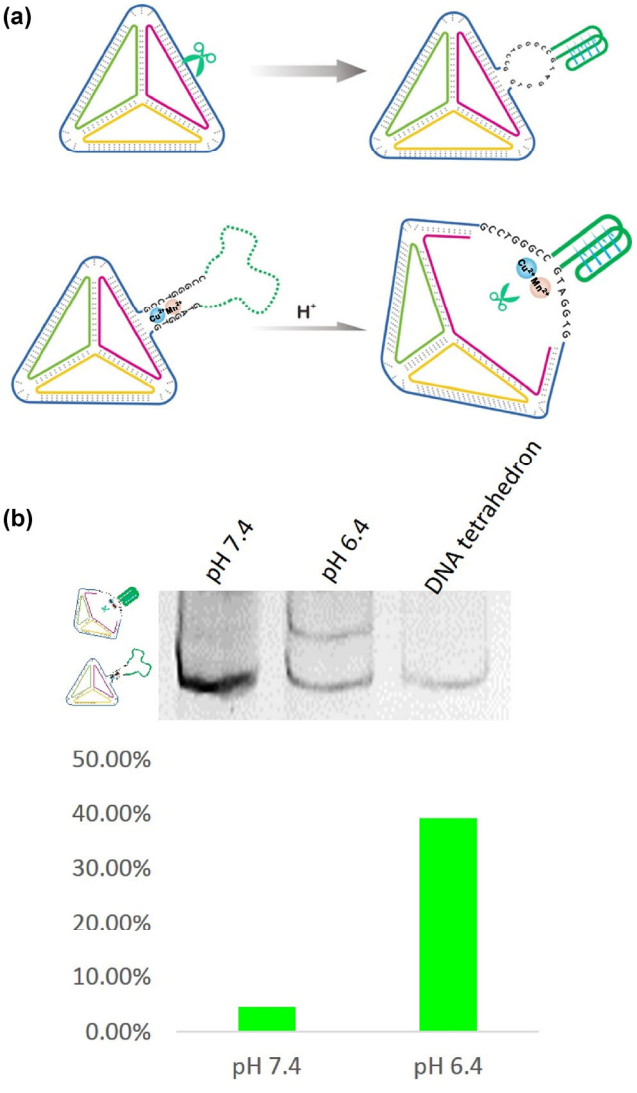

Figure 5 (a) Construction and schematic of an iMNAzyme-based DNA tetrahedron. (b) Native polyacrylamide gel electrophoresis.

i-motif/triplex sequence into the DNAzyme catalytic core to form a new tunable nucleic acid-related enzyme. By changing the sequence of the inserted i-motif/triplex, the catalytic activity was regulated and transition pH could be tuned across a range of pH 5.6 to pH 7.2. Furthermore, this work represented a description of one of the first pH-driven DNA-walker devices using an iMNAzyme capable of manipulating the stepping speed to thereby adjust walker performance. This method was also capable of opening a DNA tetrahedron structure, which provided insight into the development of tools to disassemble drug-delivered DNA nanostructures. The extraordinary properties of iMNAzymes/TNAzymes allow the potential to manipulate specific DNAs for integration into diverse devices.

Acknowledgements

The authors thank the National Basic Research Program of China (973 Program) (Nos. 2012CB720600, 2012CB720603, and 2012CB720604), the National Natural Science Foundation of China (Nos. 21432008 and 81373256).

Electronic Supplementary Material: Supplementary material (experiment details, DNA sequences, gel electrophoresis) is available in the online version of this article at http://dx.doi.org/10.1007/s12274-016-1191-x.

References

[1] Breaker, R. R. DNA enzymes. *Nat. Biotechnol.* **1997**, *15*, 427–431.

[2] Breaker, R. R.; Joyce, G. F. A DNA enzyme that cleaves RNA. *Chem. Biol.* **1994**, *1*, 223–229.

[3] Carmi, N.; Balkhi, S. R.; Breaker, R. R. Cleaving DNA with DNA. *Proc. Natl. Acad. Sci. USA* **1998**, *95*, 2233–2237.

[4] Cuenoud, B.; Szostak, J. W. A DNA metalloenzyme with DNA ligase activity. *Nature* **1995**, *375*, 611–614.

[5] Flynn-Charlebois, A.; Wang, Y. M.; Prior, T. K.; Rashid, I.; Hoadley, K. A.; Coppins, R. L.; Wolf, A. C.; Silverman, S. K. Deoxyribozymes with 2'-5' RNA ligase activity. *J. Am. Chem. Soc.* **2003**, *125*, 2444–2454.

[6] Li, Y. F., Breaker, R. R. Phosphorylating DNA with DNA. *Proc. Natl. Acad. Sci. USA* **1999**, *96*, 2746–2751.

[7] Dahl, F.; Banér, J.; Gullberg, M.; Mendel-Hartvig, M.; Landegren, U.; Nilsson, M. Circle-to-circle amplification for precise and sensitive DNA analysis. *Proc. Natl. Acad. Sci. USA* **2004**, *101*, 4548–4553.

[8] Li, Y. F.; Sen, D. A catalytic DNA for porphyrin metallation. *Nat. Struct. Biol.* **1996**, *3*, 743–747.

[9] Sheppard, T. L.; Ordoukhanian, P.; Joyce, G. F. A DNA enzyme with N-glycosylase activity. *Proc. Natl. Acad. Sci. USA* **2000**, *97*, 7802–7807.

[10] Zhang, Z. X.; Balogh, D.; Wang, F. A.; Willner, I. Smart mesoporous SiO_2 nanoparticles for the DNAzyme-induced multiplexed release of substrates. *J. Am. Chem. Soc.* **2013**, *135*, 1934–1940.

[11] Liu, J. W.; Lu, Y. A colorimetric lead biosensor using DNAzyme-directed assembly of gold nanoparticles. *J. Am. Chem. Soc.* **2003**, *125*, 6642–6643.

[12] Santiago, F. S.; Lowe, H. C.; Kavurma, M. M.; Chesterman, C. N.; Baker, A.; Atkins, D. G.; Khachigian, L. M. New DNA enzyme targeting Egr-1 mRNA inhibits vascular smooth muscle proliferation and regrowth after injury. *Nat. Med.* **1999**, *5*, 1264–1269.

[13] Elbaz, J.; Lioubashevski, O.; Wang, F. A., Remacle, F.; Levine, R. D.; Willner, I. DNA computing circuits using libraries of DNAzyme subunits. *Nat. Nanotechnol.* **2010**, *5*, 417–422.

[14] Kahan-Hanum, M.; Douek, Y.; Adar, R.; Shapiro, E. A library of programmable DNAzymes that operate in a cellular environment. *Sci. Rep.* **2013**, *3*, 1535.

[15] Elbaz, J.; Shimron, S.; Willner, I. pH-triggered switchable Mg^{2+}-dependent DNAzymes. *Chem. Commun.* **2010**, *46*, 1209–1211.

[16] Webb, B. A.; Chimenti, M.; Jacobson, M. P.; Barber, D. L. Dysregulated pH: A perfect storm for cancer progression. *Nat. Rev. Cancer* **2011**, *11*, 671–677.

[17] Mokany, E.; Bone, S. M.; Young, P. E.; Doan, T. B.; Todd, A. V. MNAzymes, a versatile new class of nucleic acid enzymes that can function as biosensors and molecular switches. *J. Am. Chem. Soc.* **2010**, *132*, 1051–1059.

[18] Phan, A. T.; Mergny, J. L. Human telomeric DNA: G-quadruplex, i-motif and Watson–Crick double helix. *Nucleic Acids Res.* **2002**, *30*, 4618–4625.

[19] Roberts, R. W.; Crothers, D. M. Specificity and stringency in DNA triplex formation. *Proc. Natl. Acad. Sci. USA* **1991**, *88*, 9397–9401.

[20] Wang, M. Q.; Zhang, H. F.; Zhang, W.; Zhao, Y. Y.; Yasmeen, A.; Zhou, L.; Yu, X. Q.; Tang, Z. *In vitro* selection of DNA-cleaving deoxyribozyme with site-specific thymidine excision activity. *Nucleic Acids Res.* **2014**, *42*, 9262–9269.

[21] Tian, Y.; He, Y.; Chen, Y.; Yin, P.; Mao, C. D. A DNAzyme that walks processively and autonomously along a one-dimensional track. *Angew. Chem., Int. Ed.* **2005**, *44*, 4355–4358.

[22] Wang, C. Y.; Tao, Y.; Song, G. T.; Ren, J. S.; Qu, X. G. Speeding up a bidirectional DNA walking device. *Langmuir* **2012**, *28*, 14829–14837.

[23] Walsh, A. S.; Yin, H. F.; Erben, C. M.; Wood, M. J. A.; Turberfield, A. J. DNA cage delivery to mammalian cells. *ACS Nano* **2011**, *5*, 5427–5432.

[24] Erben, C. M.; Goodman, R. P.; Turberfield, A. J. Single-molecule protein encapsulation in a rigid DNA cage. *Angew. Chem., Int. Ed.* **2006**, *45*, 7414–7417.

[25] Liu, Z. Y.; Li, Y. M.; Tian, C.; Mao, C. D. A smart DNA tetrahedron that isothermally assembles or dissociates in response to the solution pH value changes. *Biomacromolecules* **2013**, *14*, 1711–1714.

[26] Liu, Z. Y.; Tian, C.; Yu, J. W.; Li, Y. L.; Jiang, W.; Mao, C. D. Self-assembly of responsive multilayered DNA nanocages. *J. Am. Chem. Soc.* **2015**, *137*, 1730–1733.